

Application of low-voltage backscattered electron imaging to the mapping of organic photovoltaic blend morphologies

This content has been downloaded from IOPscience. Please scroll down to see the full text.

2015 J. Phys.: Conf. Ser. 644 012017

(<http://iopscience.iop.org/1742-6596/644/1/012017>)

View [the table of contents for this issue](#), or go to the [journal homepage](#) for more

Download details:

IP Address: 143.167.32.195

This content was downloaded on 20/11/2015 at 14:44

Please note that [terms and conditions apply](#).

Application of low-voltage backscattered electron imaging to the mapping of organic photovoltaic blend morphologies

R C Masters¹, Q Wan¹, Y Zhou², A M Sandu³, M Dapor⁴, H Zhang², D G Lidzey⁵
and C Rodenburg¹

¹Department of Materials Science and Engineering, University of Sheffield,
Sir Robert Hadfield Building, Mappin Street, Sheffield S1 3JD, UK

²School of Physics, Trinity College, Dublin 2, Ireland

³FEI Co. Europe NanoPort, Achtseweg Noord 5, Eindhoven 5651 GG, Netherlands

⁴ECT*-FBK and TIFPA-INFN, via Sommarive 18, Trento I-38123, Italy

⁵Department of Physics and Astronomy, University of Sheffield, Hicks Building,
Hounsfield Road, Sheffield S3 7RH, UK

Email: rmasters1@sheffield.ac.uk

Abstract. With organic photovoltaic (OPV) technology moving towards commercialisation, high-throughput analytical techniques are required to study the nanoscale morphology of OPV blends. We demonstrate a low-voltage backscattered electron imaging technique in the SEM that combines a solid-state backscattered electron detector with stage biasing to produce a rapid overview of the phase-separated surface morphology of an organic photovoltaic (P3HT:PCBM) blend. Aspects of obtaining the best possible results from the technique are discussed along with the possibility of probing the sub-surface morphology by altering the primary electron beam landing energy.

1. Introduction

Organic photovoltaics (OPV), consisting of a polymer:fullerene blend, are a rapidly developing alternative to conventional photovoltaic technology [1]. Recent advancements in efficiency [2] are pushing OPV devices ever-closer to becoming a feasible option for wide-scale commercialization. It has long been accepted that the (hierarchical, and often nano-scale) morphology of the OPV blend plays a key role in defining the PCE of a given blend system [3]. In order to inform the development of more efficient and consistent devices in the future, it is therefore essential to provide fast, effective tools that can provide high-resolution morphology maps for analytical purposes.

Here we present a low-voltage imaging technique in the SEM using a solid-state backscattered electron (BSE) detector as a technique enabling rapid, easily acquired overviews of OPV morphology.

2. Experimental

We produced P3HT:PCBM blends films as described in [4]. In some cases, these films were subsequently thermally annealed (for 10 minutes at 150°C) in order to encourage the formation of a coarser phase structure more representative of those employed in actual OPV devices.

All imaging was performed using the solid state concentric backscatter (CBS) detector on a FEI Nova NanoSEM 450, at a working distance of 4 mm. The detector comprises an annular design (see



Figure 1a), split in to 4 segments of increasing radius labeled A-D. These segments can be used in any combination, in order to optimize the quality of the acquired images.

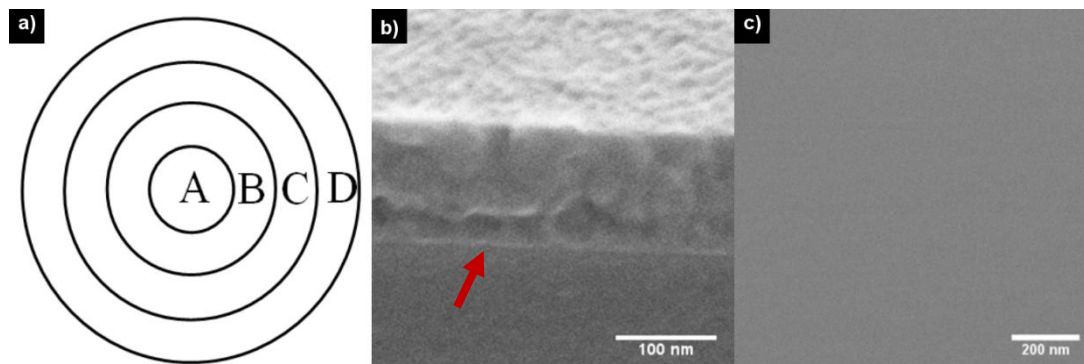


Figure 1. a) schematic of CBS detector design, b) Cross-section image of blend film as imaged in a Helium-ion microscope, used to measure blend film thickness, highlighted bright line represents the silicon-film interface. c) Example image of P3HT:PCBM blend film when using CBS detector without stage biasing.

Due to the film being relatively thin (~130 nm, as measured by helium-ion microscope cross section, Figure 1b), primary electrons with landing energies ranging from 500 eV to 3 keV were used to limit the interaction volume to the film as far as possible. Combining a solid-state BSE detector with low-energy primary beams, however, severely limits both detected signal strength (solid-state detectors have low detection efficiency below a few keV) and lateral spatial resolution in the resulting images (see Figure 1c) [5]. Applying stage biasing as a beam deceleration field has been shown to significantly improve image quality in this regard [5], by both increasing the number of electrons incident upon the CBS detector and improving the electron detection efficiency. Imaging resolution is also improved at low-kV as the electron beam is produced at a higher energy (giving inherently better resolution) before being decelerated to the desired landing energy. All images in this work have therefore used a -4kV specimen bias acting as a beam deceleration field.

3. Surface-level morphology data

To acquire surface-level morphology data, a beam landing energy of 500 eV was used in order to minimize the interaction volume of the beam. As an approximation, simplified models run in CASINO [6] suggest a maximum BSE interaction depth of ~8nm at 500 eV. Surface morphology images taken of P3HT:PCBM blend films are presented in Figure 2. We note that if a fresh blend film is imaged in this way, limited contrast is seen, which we have previously found to result from a P3HT-rich surface layer obscuring the blend morphology beneath [4]. This layer can be removed by a 5-minute low-power plasma etch in air using the FEI Nova's in-chamber procedure.

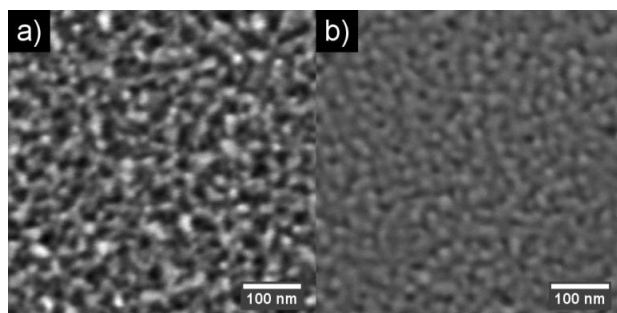


Figure 2: P3HT:PCBM blends imaged using CBS detector (segment A) at 500 eV landing energy. a) has been subject to a thermal anneal, b) is an as-cast film. The focus in both images here has been optimized; the lack of sharpness in b) is specific to the as-cast film.

We imaged P3HT:PCBM films both as-cast and after a thermal anneal. Clearly, the morphological difference between these two films can be observed in Fig. 2, with the thermally annealed sample

displaying well-defined, clear phase separation and the as-cast film showing significantly reduced contrast between phases with less definition. We have measured the lateral resolution as 8.5nm in Figure 2a using the SMART-J plugin [7] for ImageJ, which we note is inferior to the current best-resolution techniques [5,6]. However this is to be expected – the use of BSE in this technique will limit the available resolution. Nonetheless, the results appear competitive with those acquired from bright-field TEM experiments [9] whilst negating the need for an electron-transparent specimen.

4. Effect of changing the primary beam landing energy

By increasing the primary beam landing energy, the interaction volume of the beam will increase, and BSE will originate from greater depths within the film. Imaging a blend film with a range of primary beam landing energies therefore allows the subsurface structure to be probed. Figure 3 shows the effect of increasing the beam energy from 500 eV to 3 keV on an as-cast P3HT:PCBM film - an increase from ~8 nm to ~130 nm in maximum BSE escape depth. A coarsening of the imaged morphology can be observed as the landing energy is increased. We interpret this as being representative of averaged contrast between the two phases projected over gradually increasing depths through the film, although some coarsening is due to the increased lateral extent of the interaction volume (up to 100 nm at 3keV, compared to ~10 nm at 500 V, according to CASINO simulations). This also affects the imaging resolution, which may explain the loss of image clarity at higher kV. We also note the generally reduced image quality in Figure 3 in comparison to Figure 2 – no plasma clean process was used for Figure 3 in order to remove the possibility of this affecting the results.

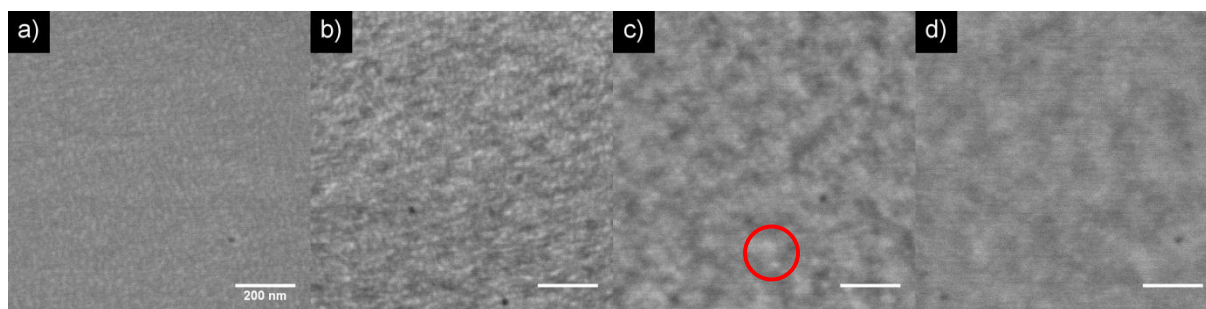


Figure 3: Thermally-annealed P3HT:PCBM film (150°C for 10 minutes) imaged using all annuli of the CBS detector using a) 500 eV, b) 1 keV, c) 2 keV (with high-contrast region highlighted), and d) 3 keV primary electron beam landing energy

Our interpretation of Figure 3 is thus: at 500 eV, the beam penetrates only the top few nm of the film. It is likely therefore that the P3HT ‘capping layer’ will have a significant masking effect on the imaged morphology as a relatively high fraction of the signal will originate from this layer. Using a 1kV primary beam, the majority of the signal originates from below the capping layer, as such the blend morphology is observed more clearly. The imaged morphology also appears coarser, perhaps representing the nature of the morphology at greater depths. At 2kV, whilst contrast between blend phases is still clearly visible, the phase structure is far less defined and is coarser still than that in Figure 3b. This partly results from some of the BSE signal originating from depths greater than the size of one phase –the BSE signal at a point on the surface has been projected through both P3HT and PCBM material. Very few areas (example circled) still show strong contrast, representing pure phases with a large surface depth (ideal for OPV morphology[10]). Hence for the given film thickness and materials, a 2 keV beam appears well suited to probe the suitability of an OPV morphology in terms of pure phases extending over a large surface depth. Using a 3 keV beam landing energy, the contrast has almost disappeared apart from some larger-scale features that we hypothesize could represent film thickness variations that alter the proportion of the BSE signal originating from the silicon substrate. Further work is required to develop these conclusions, and verify that this data is indeed reflective of the blend morphology as a function of depth. However we believe our study shows that film morphology variation can be explored by varying the landing energy of the primary beam.

4.1. Imaging considerations, optimisation of images at larger primary beam landing energies

We have found that beam optimization (i.e. stigmators, focus) can be challenging when using this technique, but if proper care is taken the image quality obtainable, in terms of signal-to-noise ratio and resolution, is more than adequate for our purposes at low-kV. We do note however that some image distortion can be found in the data at higher magnifications (field widths <1 μ m).

At beam energies above 1keV, the image signal spreads from the A to the B annulus on the CBS detector, an effect confirmed by modeling [11] of the BSE emissions from P3HT, shown in Figure 4a. Here we plot the relative BSE signal across the angular range for the CBS detector. It is observed that the BSE signal using a 3keV landing energy is more evenly spread across the CBS detector's acceptance range than at 1keV. The effect is most clearly observed in the image data in Figure 4b - the best results in this energy range are achieved by combining the signal from the A and B annuli.

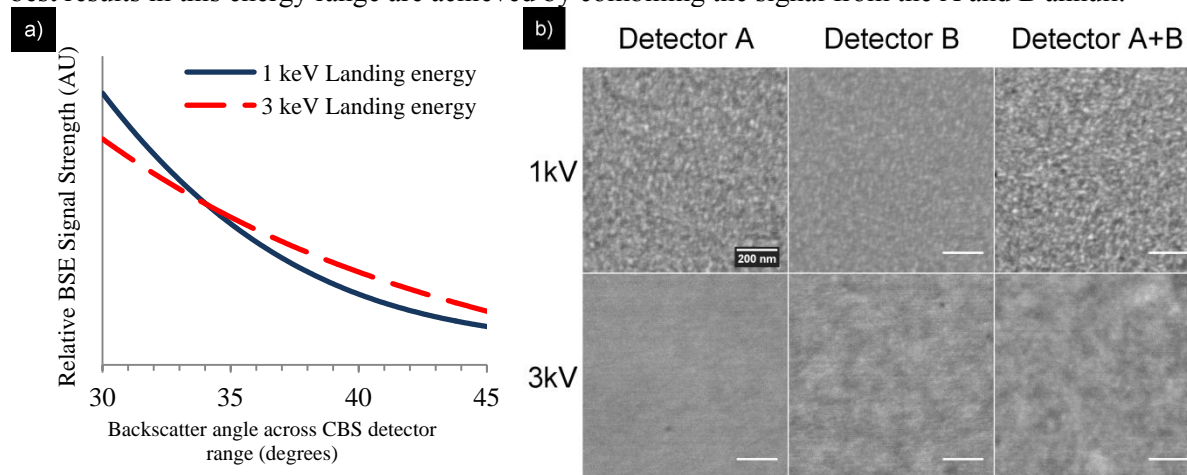


Figure 4: a) Spread of BSE signal across CBS detector at 1 keV and 3 keV; b) Variation in signal intensity between CBS detector annuli at 1 keV and 3 keV, subsequent optimization combining detectors A and B. Sample is a thermally annealed P3HT:PCBM blend, not plasma cleaned.

5. Conclusions

In conclusion, we have demonstrated a low-kV BSE imaging technique that we believe enables a rapid overview of OPV blend morphologies. By employing stage biasing to produce images with the required clarity and resolution using a solid-state BSE detector, we have been able to map nanoscale phase variation in a P3HT:PCBM blend film. The technique appears capable of displaying the key morphological differences between P3HT:PCBM blends both as-cast and subject to a thermal anneal. Most importantly, we believe that there is genuine potential for probing some aspects of the sub-surface morphology without the need for sectioning techniques.

References

- [1] Darling S B and You F 2013 *RSC Adv.* **3** 17633–48
- [2] Liu Y, Zhao J, Li Z, et al 2014 *Nat. Commun.* **5** 5293
- [3] Nelson J 2011 *Mater. Today* **14** 462–70
- [4] Masters R C, Pearson A J, Glen T S, et al 2015 *Nat. Commun.* **6** 6928
- [5] Phifer D, Tuma L, Vystavel T, et al 2009 *Microsc. Today* **17** 40–9
- [6] Drouin D, Couture A R, Joly D, et al 2007 *Scanning* **29** 92–101
- [7] Joy D C 2002 *J. Microsc.* **208** 24–34
- [8] Pfannmöller M, Flügge H, Benner G, et al 2011 *Nano Lett.* **11** 3099–107
- [9] Huang Y, Kramer E J, Heeger A J, et al 2014 *Chem. Rev.* **114** 7006–43
- [10] Moon J S, Lee J K, Cho S, et al 2009 *Nano Lett.* **9** 230–4
- [11] Dapor M 2003, *Electron-Beam Interactions with Solids; Springer Tract Mod. Phys.* (Springer).